

# Investigation on Enhancing Mesh Quality for Computational Fluid Dynamics (CFD) Analysis of an Airfoil

Ravi M Tilavalli <sup>1</sup>, G Veerabhadrappe <sup>2</sup>, Mahesh <sup>3</sup>

<sup>1</sup>*Department of Mechanical Engineering, Government polytechnic Harihara, Karnataka, India.*

<sup>2</sup>*Department of Mechanical Engineering, Government polytechnic Karatagi, Karnataka, India.*

<sup>3</sup>*Department of Mechanical Engineering, Government polytechnic Aurad, Karnataka, India.*

## ABSTRACT

Airfoils are used in many technical applications, such as aircraft, wind turbines, car spoilers, etc., to provide lift. The quality of the mesh is crucial for precise CFD analysis of airfoils, particularly when dealing with turbulent flows often seen in real-world applications. Currently, there are several technologies available for enhancing the quality of the mesh necessary for computational fluid dynamics (CFD) research. This article presents a research that aims to evaluate the impact of mesh quality on computational fluid dynamics (CFD) assessments of the NACA 23012 airfoil. The study utilizes specific open source tools for this purpose. The turbulence is simulated using the well recognized k- $\omega$  Shear Stress Transport model. In order to validate the findings, they were compared with experimental datasets collected from the "TAG Stuttgart #1" tunnel.

**Keywords:** Airfoil, Mesh Quality, AOA, Computational Fluid Dynamics, Mach number.

## 1. INTRODUCTION

Airfoils are being used in a broad variety of technical applications, including but not limited to aircraft, wind turbines, vehicle spoilers, and many more. One of the most important functions of the wing is to provide an adequate amount of lift force, often known as lift (L). For the majority of engineering applications that are dependent on the lift (L) to drag (D) ratio, it is vital to simulate the aerodynamic performance of airfoils at various angles of attack (AOA). Researchers and industry are increasingly relying on computational fluid dynamics (CFD) simulations as a result of advancements in computer hardware technology and parallel methods.

For the purpose of this investigation, the airfoil NACA 23012 [1] was selected, and the chord length of the airfoil was set at one meter. Due to its good aerodynamic performance at low flight velocities, the NACA 23012 is an attractive candidate for various computational fluid dynamics (CFD) calculations. Both the maximum lift coefficient ( $C_{Lmax}$ ) and the stall

angle ( $\alpha_{\text{stall}}$ ) are elevated as a result of its development. In accordance with the information provided in reference [1], its geometric properties are as follows:

- i) Thickness: 12%
- ii) The maximum thickness is located at the point of 30%.
- iii) The maximum chamber concentration is 1.83%.
- iv) The maximum position of the chamber is 13%.

In this study, the incompressible Reynolds-Averaged Navier-Stokes (RANS) equations are numerically approximated by utilizing the open source finite volume solver OpenFOAM [2]. This provides a more accurate representation of the problems. A parametric computational fluid dynamics (CFD) investigation of the flow around a NACA airfoil has been carried out in this research. Additionally, the impact of mesh quality on the prediction of lift and drag coefficients has been examined.

## 2. MESH QUALITY

The accuracy of the solutions obtained by computational fluid dynamics (CFD) simulations is greatly reliant on the quality of the mesh. Orthogonality, skewness, smoothness (also known as uniformity, growth factor, growth rate, or change in cell size), and aspect ratio are some of the most important criteria to consider when talking about mesh quality metrics. There are various metrics that may be used to evaluate mesh quality. It should be brought to your attention that the current research is only conducted for scenarios that are two-dimensional.

In accordance with reference [3] - "skewness has an adverse effect on the accuracy of interpolation on the face, non-orthogonality increases the error of the approximation of the surface-normal gradient, and nonuniformity reduces the order of the approximation of the surface-normal gradient to first order" . [4]–[7] are resources that readers who are interested in learning more about mesh quality and how to modify these parameters for effective computational fluid dynamics analysis may consult. According to the information provided in reference [8], the following is a concise description of each parameter that has an effect on the mesh quality.

### 2.1. Non-orthogonality

There is a straightforward illustration of mesh non-orthogonality shown in Figure 1. In accordance with the definition, mesh non-orthogonality is defined as the angular departure of the vector  $S$ , which is situated at the face center  $f$ , from the vector  $d$  that connects the two

neighboring cell centers P and N. Due to the fact that it introduces diffusion into the solution, mesh non-orthogonality mostly has an effect on the diffusive terms [8].

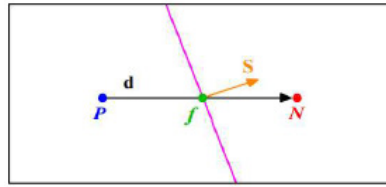


Fig. 1 Mesh Orthogonality

### 2.2. Skewness

Mesh skewness is defined as the departure of the vector  $d$  that links the two neighboring cells, such as P and N, from the face center,  $f$ , as seen in Figure 2. This particular definition is derived from the reference [8]. To a large extent, it contributes to the dispersion of the solution and has an effect on the convective terms of the remedy [8].

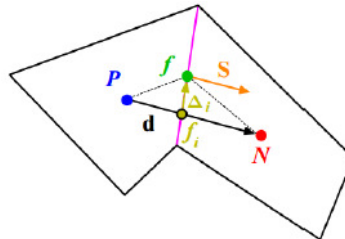


Fig. 2 Mesh Skewness

### 2.3. Smoothness

The ratio of the transition in size between cells is often referred to as smoothness. Smoothness is also known as expansion rate or growth rate. Further explanation is provided in Figure 3, which can be found here. Diffusion is introduced into the solution when there is a large transition ratio between cells [8].

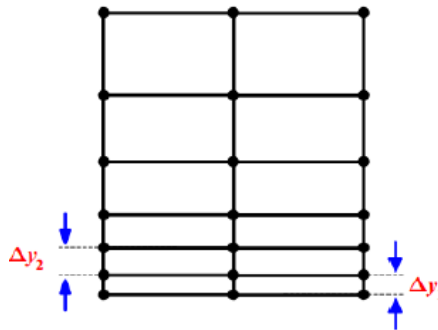


Fig. 3 Smoothness

### 2.4. Aspect Ratio

The ratio between the values of  $\Delta x$  and  $\Delta y$  is the mesh aspect ratio, as seen in Figure 4. A high AR will cause the gradients to get smeared, and as a result, it will contribute numerical diffusion to the solution [8].

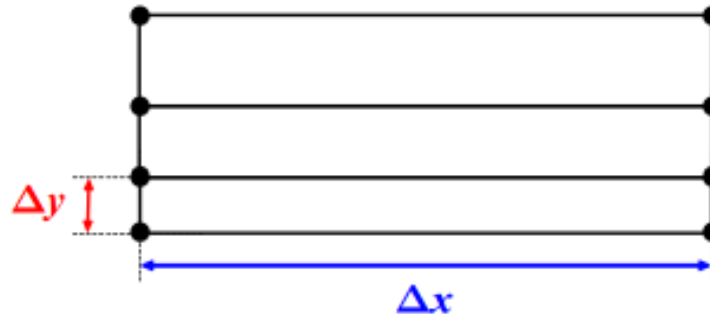


Fig. 4 Mesh Aspect Ratio

### 3. METHODOLOGY

In order to demonstrate the significance of mesh quality on the correctness of the solution, we carried out a parametric analysis with the use of open source computing tools. In Figure 5, we see the various phases of the research as well as the technologies that were used.

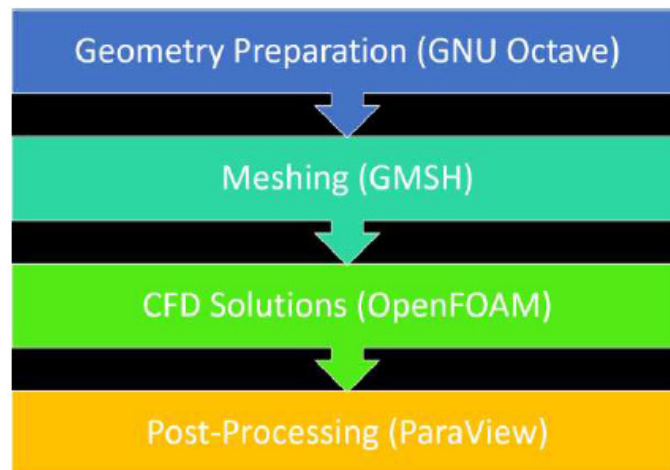


Fig. 5 Methodology of investigation

#### 3.1. Meshing

Finally, the geometrical data file that was produced by the script is used in the process of mesh generation by means of an open-source program known as GMSH [11]. It is possible to convert the mesh files from GMSH into the OpenFOAM mesh format by using the "gmshToFoam" command inside the OpenFOAM environment during the conversion process. The input factors that have the potential to change the meshes' quality are shown in Tables 1 and 2, respectively. There have been a great number of meshes with a variety of characteristics that have been researched, and only the ones that were chosen are provided in

these tables. Following the completion of the mesh preparation process, the quality of each mesh was evaluated by using the "checkMesh" function in OpenFOAM. The most important factors that are associated with quality are shown in Tables 1 and 2.

**Table 1: Input and output for Gmsh for AOA = 0°**

Mesh ID	Inputs				Outputs			
	bump	N1	N2	N3	N4	Maximum aspect ratio	Maximum Non-orthogonality	Maximum skewness
M13	1	400	40	30	30	665.06	69.25	1.35
M14	1	500	40	30	30	664.88	69.25	1.35
M19	10	500	40	30	30	664.88	75.90	2.85
M20	20	500	40	30	30	664.88	78.29	3.58
M21	30	500	40	30	30	664.88	79.29	4.04
M22	0.0001	500	40	30	30	664.8795	78.28	4.28
M23	0.001	500	40	30	30	664.8795	76.11	3.01
M24	0.01	500	40	30	30	664.8795	71.62	1.75

**Table 2: Input and output for Gmsh for AOA = 10°**

Mesh ID	Inputs				Outputs			
	bump	N1	N2	N3	N4	Maximum aspect ratio	Maximum Non-orthogonality	Maximum skewness
U14	1	500	40	30	30	665.1764	71.95165	1.7937
U15	1	500	40	30	30	332.5241	70.41457	1.867064
U16	1	500	40	30	30	3325.454	73.03355	1.908497
U17	1	500	40	30	30	1662.638	73.38908	1.817821
U18	1	500	40	30	30	1109.237	73.68965	1.838289
U19	1	500	40	30	30	169.8483	69.90738	1.27191
U20	1	500	40	30	30	169.8483	70.11737	1.334913
U22	0.0001	500	40	30	30	665.1764	78.28807	4.288395
U30	0.0001	500	40	30	30	332.5241	81.46802	4.287458

The output characteristics, which include maximum aspect ratio (AR), maximum non-orthogonality, and maximum skewness of mesh, have been taken into consideration in order to ascertain the quality of the mesh. In order to have the best possible mesh, the maximum AR

should be as near to 1 as feasible, and the maximum skewness should be as low as possible. In addition, the maximum non-orthogonality of the mesh should be lower than 70 percent.

We simulated the high quality mesh scenario (Mesh ID: M14 and U14) as well as the poor quality mesh case (Mesh ID: M22 and U22), and then we compared the aerodynamic coefficients that were generated by the simulation to the data that was obtained from experiments [12].

### **3.2. CFD Solutions**

For the purpose of this investigation, we made use of the open-source numerical package OpenFOAM version 3.0.1 [2], which is a method for solving collocated unstructured finite volume problems. A Linux (Ubuntu 14.04 LTS) platform with four processors, a maximum speed of 2.59GHz, and a total of 12GB of RAM memory was used to power the computational fluid dynamics (CFD) instances. When modeling turbulence, we used the  $k-\omega$  SST turbulence model developed by Menter, which has been well verified, and included wall functions [13]. The flow is supposed to be an incompressible subsonic flow, and the turbulence intensity (TI) is supposed to be set to 0.02%. The Reynolds Number (Re) is supposed to be  $1 \times 10^6$ , and the Mach Number (M2) is supposed to be 0.04. The instances are successfully resolved by using the unbounded gradient discretization technique of the second order. A procedure that is at least second order correct in space is used in order to solve each and every one of the cases that are mentioned in tables 1 and 2. till the quantities of interest did not exhibit any oscillations, the cases were ran till they were finished.

### **3.3. Post-processing**

Following the completion of the OpenFOAM analysis, the findings were evaluated using the post-processing program known as ParaView [14]. In addition, the amount of interest was plotted using GNUplot [15], which included the residuals, lift and drag coefficients, and other relevant parameters.

The line-integral convolution method (LIC), which was developed in ParaView [14], was used by us in order to demonstrate the wake topology. Through the use of this method, high density streamline charts may be generated in a two-dimensional visualization [16]. Because of its visualization characteristic of condense lines, which depicts the evolution of wake structure much more clearly, the LIC approach is more desirable than the typical streamlines technique in this research. This is because the LIC technique provides a more accurate representation of wake topology.

#### 4. RESULTS AND DISCUSSION ANALYSIS

The current research examined many meshes at angle of attack (AOA) values of  $0^\circ$  and  $10^\circ$ . The mesh that demonstrated the highest quality and ability to accurately represent the involved physics was chosen for further examination at various AOA values. The simpleFoam solver, which employs the SIMPLE method for pressure-velocity coupling, was used for conducting the steady flow simulations. The findings acquired using OpenFOAM are compared to experimental data derived from a research conducted at Stuttgart Tunnel #1, as referenced in [12]. The experiment was conducted in a wind tunnel, using six different Reynold Numbers ranging from 700,000 to 3,000,000. The NACA 23012 airfoil was used, with a turbulence intensity (TI) of 0.02%.

In order to align with the experimental data, the appropriate turbulence-related parameters were computed for a turbulence intensity of 0.02% in OpenFOAM. Tables 3 and 4 provide the aerodynamic coefficient of the examined case studies.

**Table 3: Aerodynamic coefficient for cases AOA =  $0^\circ$**

<b>Aerodynamic Coefficient</b>	<b>M14</b>	<b>M22</b>	<b>Experimental [12]</b>
<b>Lift Coefficient (<math>C_L</math>)</b>	0.1271	0.03116	0.15
<b>Drag Coefficient (<math>C_D</math>)</b>	0.01203	0.01113	0.0071

**Table 4: Aerodynamic coefficient for cases AOA =  $10^\circ$**

<b>Aerodynamic Coefficient</b>	<b>U14</b>	<b>U22</b>	<b>Experimental [12]</b>
<b>Lift Coefficient (<math>C_L</math>)</b>	1.0501	0.9388	1.13
<b>Drag Coefficient (<math>C_D</math>)</b>	0.02447	0.02007	0.0156

The investigations M14 and U14 use high-quality mesh for the AOA= $0^\circ$  and AOA= $10^\circ$  situations, respectively, as previously stated. The acquired findings closely corresponded to the experimental results. Furthermore, it is evident that although the drag coefficient has no impact, there is a substantial disparity in the lift coefficient. The current work used a wall function to accurately simulate the boundary layer around the NACA airfoil. Nevertheless, accurately simulating drag forces for airflow across airfoils in CFD analysis is a complex task, and more accurate outcomes may be achieved by using transition and turbulence models.

Figures 6 and 7 show the convergence of the coefficient of drag ( $C_D$ ) and coefficient of lift ( $C_L$ ) values in the investigation. It is evident that a higher-quality mesh, namely M14

and U14 (shown by the red line), achieves quicker convergence at about 500 time-steps in comparison to M22 and U22.

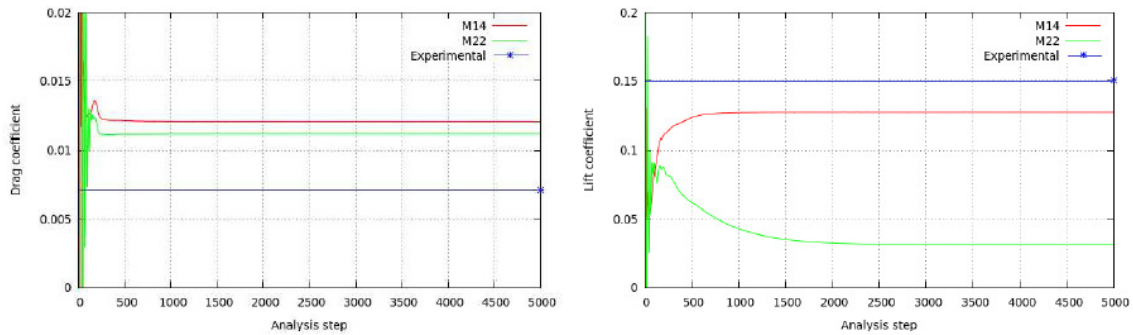


**Fig 6 Convergence of the CD and CL value for case AOA=0° over time steps and comparison to the experimental data**

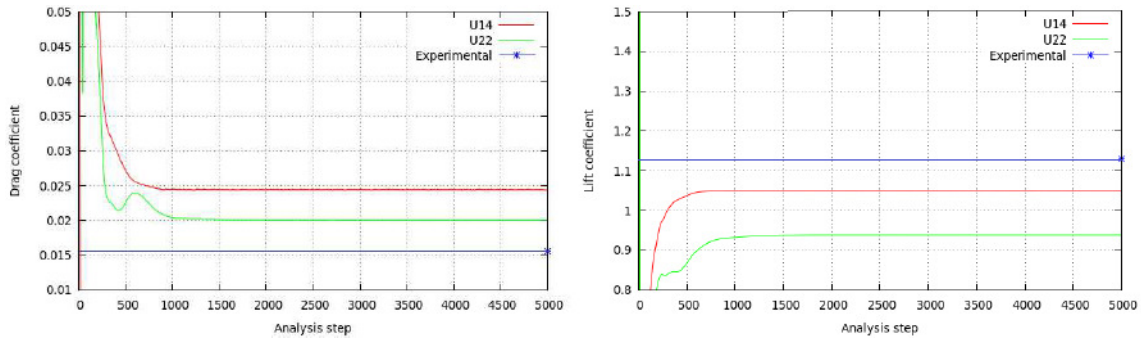


**Fig. 7 Convergence of the CD and CL value for case AOA=10° over time steps and comparison to the experimental data**

The M14 and U14 examples exhibited shorter run times compared to both the M22 and U22 instances, although having the same computing capabilities and flow solution. This demonstrates that when using a mesh of poor quality, it is probable to get satisfactory outcomes, but at the expense of longer computational time. It is important to note that non-orthogonality, skewness, and non-uniformity only pose issues in areas where there is a significant change in gradient. Thus, in this particular scenario, the quality of the mesh has little impact on the drag value across all four situations.

Figures 8 and 9 show the outcome of the post-processing analysis for both cases of AOA=0° and AOA=10° using the Line-integral Convolution (LiC) visualization approach. There is no wake structure found in any of the situations.



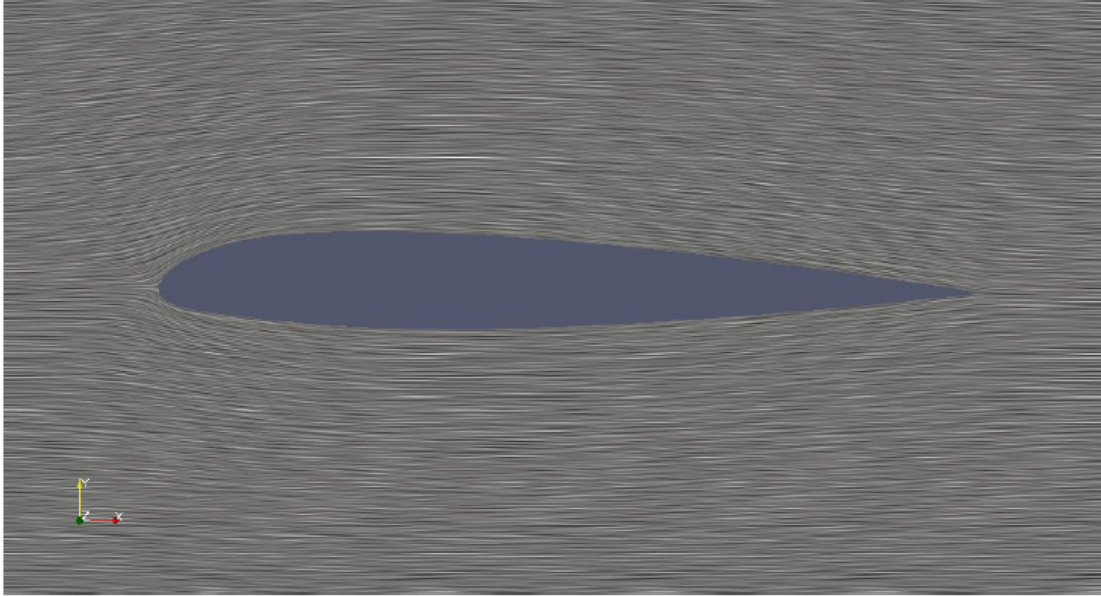


**Fig. 8 LiC visualization for case AOA = 0°**

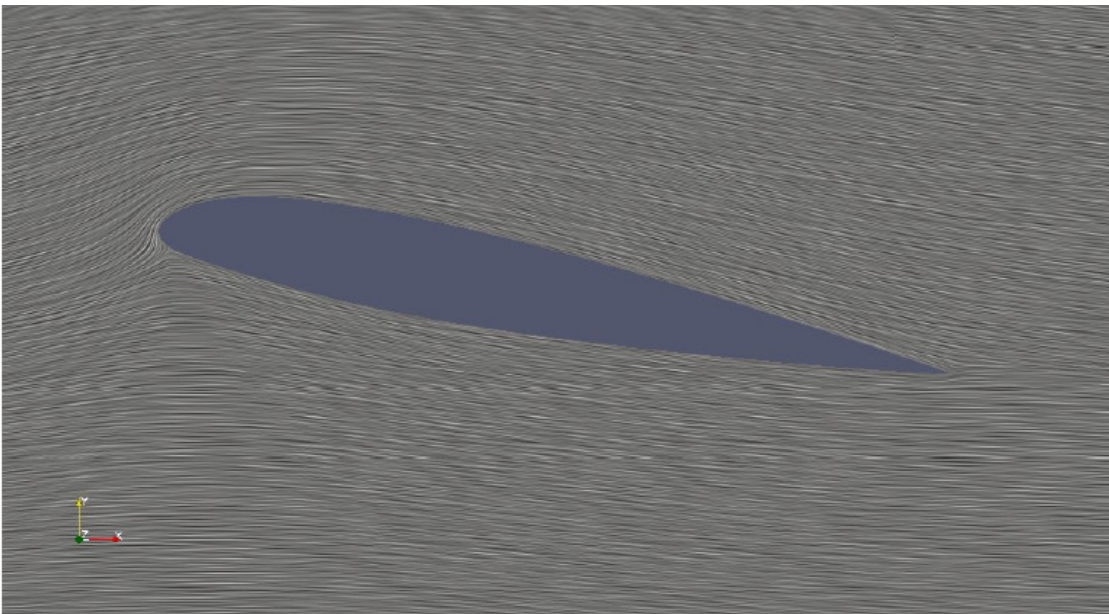


**Fig. 9 LiC visualization for case AOA = 10°**

## **5. CONCLUSIONS**

In light of the findings of the study, the following assessments have been made. CFD and MODAL analysis were performed on a wide variety of aerofoils, each of which had a varied thickness expressed as a percentage of chord. In terms of lift to drag values, it was discovered that the Wortmann fx63-137 has the optimum values when the angle of attack is 12 degrees and the Mach number ranges from 0.2 to 0.6. According to the findings that were acquired using ANSYS FLUENT, it has been discovered that the wortmann fx63-137 has the most

favorable pressure and velocity distributions among the many airfoils that were considered. With the use of the XFLR5 program, we created graphs that contrasted  $C_l$  with  $C_d$ ,  $C_l/C_d$  with  $\alpha$ , and  $C_m$  with  $\alpha$ . Figure illustrates the comparison between a number of different airfoils. It has been discovered that Wortmann fx63-137 has the maximum  $C_l$  value when the  $C_d$  level is low. Based on the results of the modal analysis, the material wortmann and clark y has the highest resistance to stretching and stresses.

## REFERENCES

1. The Foam House [<http://the-foam-house5.webnode.es/products/chapter-4-airfoil-case/>]
2. OpenFOAM [<https://www.openfoam.com>]
3. Juretić F. and Gosman A. D. (2010) Error Analysis of the Finite-Volume Method with Respect to Mesh Type. *Numer. Heat Transf. Part B Fundam.*, 57(6): 414–439.
4. Juretic F. (2004) Error analysis in finite volume CFD. PhD thesis, University of London, Department of Mechanical Engineering.
5. Knupp P. M. (2008) Remarks on mesh quality, 46th AIAA Aerospace Sciences Meeting and Exhibit.
6. Katz A. and Sankaran V. (2011) Mesh quality effects on the accuracy of CFD solutions on unstructured meshes, *J. Comput. Phys.*, 230(20):7670–7686.
7. Baker T. J. (2005) Mesh generation: Art or Science?, *Prog. Aerosp. Sci.*, 41(1):29–63.
8. OpenFOAM Introductory Course Material: Module 3. [<http://www.wolfodynamics.com/ourservices/training/openfoam-intro-raining.html?id=50>].
9. GNU Octave [<https://www.gnu.org/software/octave/about.html>].
10. Airfoil simulations - A little contribution for meshing [<http://codesaturne.org/forum/viewtopic.php?f=10&t=957>].
11. Gmsh: A three-dimensional finite element mesh generator with built-in pre- and postprocessing facilities [<http://geuz.org/gmsh/>].
12. Miley S. J. (1982) A Catalog of Low Reynolds Number Airfoil Data for Wind Turbine Applications”, Prepared by Department of Aerospace Engineering, Texas A&M University for Rockwell International Corporation, USA.
13. Menter F. R., Kuntz M., and Langtry R. (2003) Ten Years of Industrial Experience with the SST Turbulence Model, *Turbul. Heat Mass Transf.*, 4:625–632.
14. ParaView [<https://www.paraview.org>].
15. GNUplot [<http://www.gnuplot.info>].
16. Knowles R. D., Finnis M. V., A. J. Saddington, and Knowles K. (2006) Planar visualization of vortical flows, *Proc. Inst. Mech. Eng. Part G J. Aerosp. Eng.*, 220(6): 619–627.

17. Jithendra Sai raja chada, Sri ram deepak akella et. Al : Study Of Flow Characteristics In a Convergent And Divergent Nozzle Using Computational Fluid Dynamics International Journal of Scientific Research and Engineering Development— Volume 4 Issue 3, May -June 2015.
18. K. M. Pandey, S. K.Yadav : CFD Analysis of a Rocket Nozzle with Four Inlets at Mach 2.1 International Journal of Chemical Engineering and Applications, Vol. 1, No. 4, December 2010 ISSN: 2010-0221.
19. K. M. Pandey and Virendra Kumar : CFD Analysis of Four Jet Flow at Mach 1.74 with Fluent Software International Journal of Chemical Engineering and Applications, Vol. 1, No. 4, December 2010 ISSN: 2010-0221.
20. Kousik kumaar. R, kesavan.M : Design and cfd analysis of shock waves over supersonic cd nozzle international journal of latest trends in engineering and technology (IJLTET) ISSN:2278-621X, p-502 to510.
21. Arun Kurien Reji, G. Kumaresan, Archit S Menon, Jithesh Parappadi, Harikrishna A. P, Ajaykrishnan Mukundan International Journal of Pure and Applied Mathematics Volume 119 No. 12 2016, 2135-2142.
22. H Pujowidodo, A I Siswantara2, G G R Gunadi. : A Daryus The Study of Converging-Diverging Nozzle for Improving the Impulse Momentum of Cross-Flow Turbine in a Bio-Micro Power Plant ICB2018 IOP Conf. Series: Earth and Environmental Science 209 (2018) 012054 IOP Publishing doi:10.1088/1755-1315/209/1/01205.
23. Gamble, Dwain Terrell, P.E. Rich DeFrancesco : Nozzle selection and design criteria AIAA-2004-3923.
24. E. M. S. Ekanayake, J. A. Gear, Y. : Ding Flow simulation of a two dimensional rectangular supersonic convergent-divergent nozzle ANZIAM J. 51 (EMAC2009) (page number C377–C392), 2010.
25. Mhammad Arif Hussain, M.Satya Prasad, Dr. S.Nagakalyan : Design and flow analysis of various convergent - divergent nozzles by using computational fluid dynamics (CFD)- International Journal of Innovative Research in Advanced Engineering (IJIRAE) ISSN: 2349-2163 Issue 05, Volume 6 (page number 372 to 379) doi://10.26562/IJIRAE.2019.MYAE10087.
26. Bogdan-Alexandru Belega, Trung Duc Nguyen : Analysis of flow in convergent-divergent rocket engine nozzle using computational fluid dynamics -international conference OF scientific paper afases Brasov, 28-30 May 2015.
27. Raghu Ande, Venkata N. Kumar Yerraboina Numerical Investigation on Effect of Divergent Angle in Convergent-Divergent Rocket Engine Nozzle-chemical engineering transactions vol. 66, 2018 from (page number 787 to 792) DOI: 10.3303/CET1866132.